Available online at www.sciencedirect.com
SCIENCE DIRECT
Polymer 47 (2006) 577–584
polymer
www.elsevier.com/locate/polymer

The application of attenuated total reflectance Fourier transform infrared spectroscopy to monitor the concentration and state of water in solutions of a thermally responsive cellulose ether during gelation

Chris Sammon [a,*], Gurjit Bajwa [b], Peter Timmins [c], Colin D. Melia [b]

[a] *Materials and Engineering Research Institute, Sheffield Hallam University, City Campus, Howard Street, Sheffield S1 1WB, UK*
[b] *Formulation Insights, School of Pharmaceutical Sciences, University of Nottingham, Nottingham NG7 2RD, UK*
[c] *Biopharmaceutics R&D, Pharmaceutical Research Institute, Bristol Myers Squibb, Moreton, Wirral CH46 1QW, UK*

Received 15 August 2005; received in revised form 17 November 2005; accepted 22 November 2005
Available online 15 December 2005

Abstract

This paper reports the use of ATR-FTIR with PLS data analysis to probe the thermal gelation behaviour of aqueous solutions of the cellulose ether, hydroxypropyl methylcellulose (HPMC). Spectroscopic changes in the ν(CO) region of the infrared spectra (collected using ATR) were shown to mark the onset of gelation and information about the temperature of gelation and the effect of the gel structure on the water hydrogen bonding network was elucidated. The use of PLS data analysis to quantify the water concentration within the gel at the ATR interface is highlighted. The dominance of intermolecular H-bonding over intramolecular H-bonding within the cellulose ether in solution was also observed. The ATR-FTIR data was in good agreement with rheological and DSC measurements conducted on the same systems. A discussion regarding the changes in shape of the ν(OH) band of the water within the gel is provided and an interpretation of these changes in terms of modifications of the hydrogen bond strength of associated water during syneresis is given.

Keywords: Cellulose ether; ATR-FTIR; Gelation

1. Introduction

The use of hydrophobically modified water soluble polymers to control the rheological properties of aqueous based systems is widespread, with the technology applied to food [1], oil recovery [2], cosmetics [3] and pharmaceuticals [4]. More esoteric studies on synthetic polymers have provided a rudimentary understanding of the link between the nature and number of hydrophobic substituents and their rheological behaviour [5]. But studies on the derivatives of natural materials are less well understood due in part to the heterogeneity of the substitution and a lack of suitable models. Kondo et al. [6–8] have tried to address this lack of understanding but, due to the similar reactivities of the OH groups at the 2 and 3 position on the cellulose backbone, the number of model compounds that can be made using their methodology is limited to 2,3-di-*O*-methylcellulose and 6-*O*-methylcellulose with different degrees of heterogeneous substitution.

The propensity of HPMC (shown in Fig. 1) and certain other cellulose ethers, to undergo a reversible sol–gel transition at elevated temperatures in aqueous solution, has been widely studied [9–13]. The heating of cellulose ether solutions eventually results in loss of solubility and a temperature is reached, at which precipitation of the polymer and/or gel formation occurs. Both solubility effects and gel formation are fully reversible, although a degree of hysteresis can occur, and are reproducible, irrespective of the thermal history of the sample [14]. Gelation of HPMC is thought to arise from increasing hydrophobic interactions and exclusion of water (syneresis) from heavily methoxylated regions of the polymer [15]. In contrast, hydroxypropyl cellulose (HPC), a closely related material that does not contain methoxyl substituents, precipitates on heating but does not form a gel [16,17]. It has also been observed that methylcellulose has a lower gelation temperature and formed firmer gels than HPMC of equivalent substitution and molecular weight, indicating that hydroxypropyl substituents inhibit gelation [18,19].

* Corresponding author. Tel.: +44 114 2253890.
E-mail address: c.sammon@shu.ac.uk (C. Sammon).

0032-3861/$ - see front matter © 2005 Elsevier Ltd. All rights reserved.
doi:10.1016/j.polymer.2005.11.067

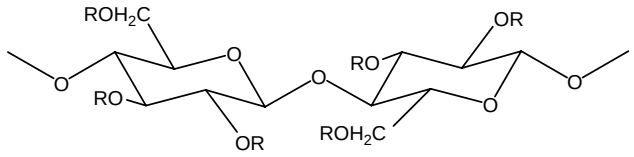

Hydroxypropylmethylcellulose R = H, CH_3, $CH_2CH(OH)CH_3$

Fig. 1. Chemical structure of the cellulose ether used for this study.

ATR-FTIR has become a very important tool for characterising hydrogen bonding in aqueous systems [20–22] and determining the interactions between sorbed water and polymer matrices [23–25]. The detailed theory of attenuated total reflectance Fourier transformed infrared spectroscopy (ATR-FTIR) is available elsewhere [26] but it is worth summarising the salient points in relation to this paper. The most important feature of the ATR experiment is the evanescent field, which develops during the reflection of radiation at the interface of a material with a high refractive index (ATR crystal, n_2) and a material with a low refractive index (sample, n_1). Attenuation of this electric field by functional groups in the lower refractive index material results in a spectrum analogous to an absorbance spectrum. The depth of penetration (dp) of the evanescent field is governed by the wavelength of incident radiation (λ_1), the angle of incidence (θ_{inc}) and the ratio of the ATR crystal and sample refractive indices (n_{21}). This limits the sampling depth which can be estimated using Eq (1). In practice, the effective sampling depth is considered to be $\sim$3dp.

$$\mathrm{dp} = \frac{\lambda_1}{2\pi\left(\sin^2\theta_{\mathrm{inc}} - n_{21}^2\right)^{1/2}} \tag{1}$$

As a result, the spectral information obtained will only be from the few microns close to the ATR crystal, regardless of the overall thickness of the sample. Therefore it is possible to obtain spectra from very strongly absorbing materials including water.

FTIR has been used to characterise the gel structure of a number of systems including synthetic polymers [27,28], proteins [29,30] and starches [31–34]. Iizuka and Aishima [31] used ATR-FTIR spectroscopy with evolved factor analysis to obtain information about the gelation processes of corn and potato starch. They reported profound intensity changes in the ν(CO) region of starch solutions during gelation and postulate that this is due to changes in the interaction of water with starch granules between 74 and 80 °C. Wilson et al. [32] and Bilkin et al. [33] used ATR-FTIR to study the gelation and retrogradation of waxy-maize starch and wheat starch gels, respectively. Once more, changes in the relative intensities of bands between 1200 and 800 cm^{-1}, indicated morphological changes and correlated well with rheological measurements. Lui et al. [34] have used FTIR in transmission mode to look at phase changes in potato starch solutions. They also reported increases in the intensity of bands between 1200 and 800 cm^{-1} during gelation. The authors also indicated changes in the types and nature of molecular interactions during gelation, suggesting that gelation was a hydration process.

Ostrovskii et al. have used a transmission FTIR method to study the thermal gelation of ethyl (hydroxyethyl) cellulose in the presence of an ionic surfactant [35]. The paper included a study of the changes in the 1200–900 cm^{-1} bands before and after gelation and indicated that a band around 1075 cm^{-1}, assigned to skeletal vibrations of the saccharide rings, decreased as a function of gelation. This, they postulate, was due to the rings being 'more bound' in the gel state. Conversely a band around 1120 cm^{-1}, assigned to C–O–C bridges, increased as a function of gelation, also as a result of a decrease in mobility of the cellulose rings. The authors also report interactions with SO_3^- groups in the surfactant, but because of the relatively large cell path length (25 μm) they were unable to obtain information regarding the structure of water in the gel state.

We have previously reported the significant and reproducible increase in intensity of the ν(CO) region of aqueous K4M HPMC solutions subjected to a temperature ramp in a sealed environment [36]. We observed a dependence of the measured gel point on the concentration of polymer and reported evidence of syneresis. These results were corroborated using a light scattering methodology. This investigation applies ATR-FTIR with partial least squares (PLS) data analysis to the study of thermal gelation phenomena in HPMC solutions and builds on our previous findings for K4M grade HPMC solutions.

This paper is part of a program of work examining the relationship between molecular interactions and the physical changes (thermal transitions, turbidity changes and rheological changes) that occur in thermally-responsive cellulose ether solutions. The role played by water in the sol–gel transition is poorly understood and in principle, vibrational spectroscopy readily facilitates the probing of water structure within the polymer network. Changes in the 'state' of water, and understanding factors affecting the gelation mechanism with respect to the sol–gel transition can potentially yield important information for intelligent formulation in food, cosmetic and pharmaceutical systems. Quantifying the water within the gel state may also provide significant information with respect to the syneresis process as it is unclear whether water loss leads to stronger hydrophobic chain interactions or if polymer/polymer interactions are the driving force for the proposed redistribution of water. Elucidating information on the state of the water in these systems may lead us part way to answering this question. This paper focuses on (i) establishing the viability of the technique for such studies (ii) characterising the state of the water in the gel network and (iii) quantifying polymer chain water loss (syneresis) during the sol–gel transition.

2. Experimental

HPMC solutions (Methocel E4M CR Premium USP/EP, hydroxypropyl content 9.3% and methoxyl content 29.5%, BN OD16012N32, Colorcon Ltd, Dartford, UK) were prepared using the method of Banks et al. [36].

2.1. FTIR-ATR measurements

ATR-FTIR spectra were collected using a temperature controlled Golden Gate™ single reflection ATR accessory (SpectraTech) coupled to a ThermoNicolet Nexus FTIR spectrometer. Samples were placed in direct contact with the ATR crystal and sealed using a 'volatiles' cap to ensure no water loss during the heating and cooling runs. The samples were allowed to equilibrate for 8 min at the required temperature prior to data collection. Data were collected by averaging 64 scans at 4 cm^{-1} resolution. Both the blank ATR crystal and 18 mΩ water at the same temperature under the same conditions were used as reference backgrounds.

2.2. Rheological measurements

The dynamic viscoelastic functions (storage modulus G', loss modulus G'' and tan δ) were determined as a function of temperature using a Bohlin C-VOR (Bohlin Instruments Ltd, UK) fitted with acrylic parallel plate (40 mm) geometry. A continuous temperature sweep (10–85 °C and subsequently 85–10 °C) at a rate of 1 °C/min was undertaken. Measurements were carried out at an angular frequency of 0.5 Hz and at 5% strain to ensure the linearity of viscoelasticity. To prevent dehydration during rheological measurements, a thin layer of low-viscosity silicone oil was placed on the periphery surface of the solution held between the plates.

2.3. Micro DSC measurements

A high sensitivity differential scanning microcalorimeter (Seteram Micro DSC 3, Lyon, France) was used to determine the transition temperature of HPMC during the thermal cycle. Samples were injected by a syringe into a sample cell and 18 mΩ water was injected into a reference cell, taking care to avoid air bubbles. Prior to a series of runs, a baseline experiment was carried out by adding degassed water to each cell and scanning over the temperature range of interest. After loading and equilibrium, a heating and cooling rate equal to that employed in the rheological experiments of 1 °C/min was used, the instrument was set to record data every 0.025 °C. For the microthermal analysis, the sample underwent heating from 20 to 80 °C, and subsequently it was immediately cooled from 80 to 20 °C.

3. Results and discussion

To gain an understanding of the mechanical changes occurring in HPMC during a temperature ramp, the dynamic viscoelastic functions; storage modulus G', loss modulus G'' and tan δ (G''/G') of the polymer were measured. Rheological measurements are the most direct way for determination of the sol–gel transition and the crossover of G' and G'' (i.e. tan $\delta = 1$) has been widely used as an indication of the sol–gel transition point. The influence of temperature on sample structure was investigated over a temperature range of 10–85 °C at ramp rate

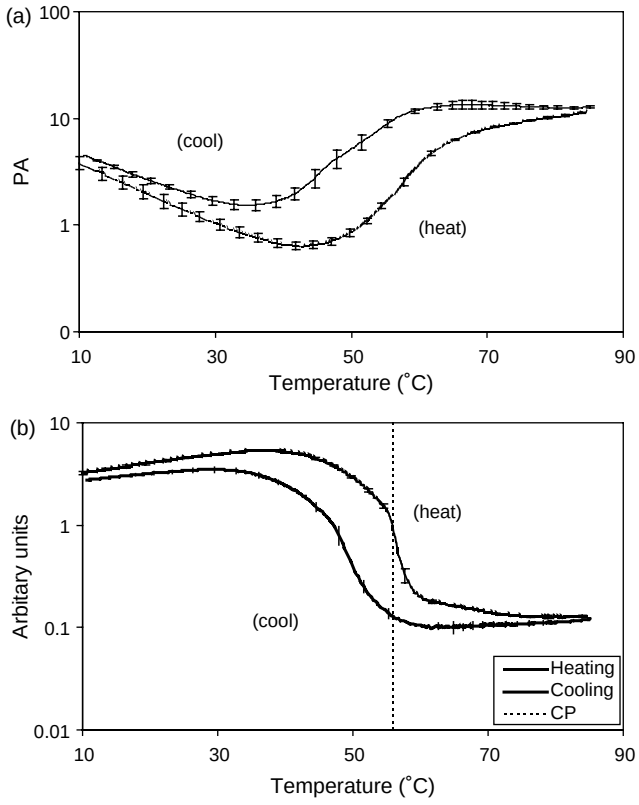

Fig. 2. Plot of (a) storage modulus (G′) versus T and (b) tan δ versus T for a 2% E4M solution, with a heating and cooling rate of 1 °C/min, a 5% oscillatory strain, and a frequency of 0.5 Hz.

of 1 °C/min. An oscillatory strain of 5% (within the linear viscoelastic region) and a frequency of 0.5 Hz were used.

Fig. 2(a) shows the plot of storage modulus (G') as a function of temperature for both the heating and cooling cycle. Below 43 °C the storage modulus progressively decreases as a function of temperature. This has been related by Haque et al. to an unbundling of native cellulosic fibres and is responsible for the increase in volume of the solution [18,19]. Above 43 °C there is a gradual increase in G' which plateaus around 65 °C. This gradual increase in elastic nature is characteristic of the progressive formation of a weak structured elastic gel, held together by weak hydrophobic interactions.

The overall thermal viscoelastic character of the sample can be obtained by plotting the ratio of the storage modulus with the loss modulus (G'/G'') or tan δ. Fig. 2(b) shows the plot of tan δ of a 2% E4M solution as a function of T for a heating and cooling run. At temperatures below the crossover point ($G' < G''$), the system exhibited common viscoelastic behaviour typical of a liquid, whereas following the crossover ($G' > G''$) a weak but elastic structure was formed. The crossover point, i.e. tan $\delta = 1$ was shown to be at 56 °C. The cooling plots measured under the same conditions with a cooling rate which matched the initial heating rate (1 °C/min) both show evidence of hysteresis. This has been explained by suggesting that the rate of disentanglement is lower than the gelation process [18], but may simply be the result of the gel structure being retained during supercooling. These results are

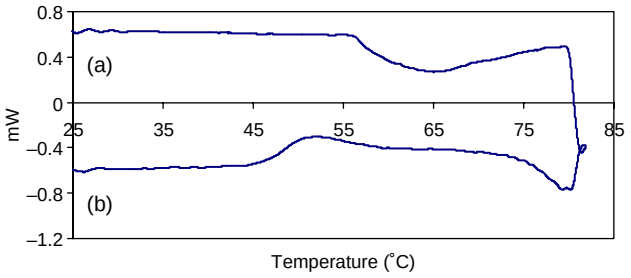

Fig. 3. Differential scanning calorimetry of a 2% E4M solution collected using a (a) heating and (b) cooling rate of 1 °C/min.

the subject of further investigation; they are included here mainly to help determine the gel point. Although the precise gel point temperature will depend on the extent of substitution in the HPMC batch being examined, the shape of the rheological profile follows closely that obtained for an E4M grade HPMC by Haque and Morris [19].

To gain an insight into the energetics of the gelation properties of E4M solutions and provide suitable confirmation of the gelation temperature using a traditional analysis method, the samples were analysed using differential scanning calorimetry (DSC). The DSC results collected during a heating and cooling regime of 1 °C/min are shown in Fig. 3. In agreement with the rheology studies, this data indicates that there is an intrinsic change in the nature of the sample at 56 °C in the heating curve, which is manifested as an endotherm in the DSC trace. In agreement with the oscillatory rheometry measurements, the cooling experiment shows evidence of hysteresis. The hysteresis pattern closely resembles that obtained for E4M HPMC by Haque and Morris [19].

It is clear that despite the value of the information provided by oscillatory rheometry and DSC, it is difficult to gain an insight into the molecular interactions that lead to the phenomena observed. In contrast, vibrational spectroscopy can readily be used to obtain information about interactions (hydrogen bonding, hydrophobic interactions) at the molecular level. Previous work has shown that the ν(CO) band (1250–900 cm^{-1}) of HPMC is highly sensitive to water content and is shown to narrow during hydration [36]. This has been explained in terms of the reduction of the number of different types of hydrogen bond in the solution compared to the 'dry' solid; with intermolecular hydrogen bonding between the hydrophilic moieties on the HPMC chains and water dominating.

Fig. 4 shows the effect of temperature on a 2% E4M solution measured using ATR-FTIR spectroscopy. It is worth commenting that this data was generated using 18 mΩ water as a reference background to remove the dominant water signal and make observations in the changes of the ν(CO) band more prominent. From Fig. 4 it is clear that the intensity of the ν(CO) band increases significantly as a function of T, as was reported previously for a different grade of HPMC; K4M [36]. This implies that during gelation the concentration of HPMC within the evanescent field is increasing. The most simple explanation is that the thermally formed gel has a higher density than HPMC solution (or water) and the geometry of the system is such that gravity forces the denser material closer to the ATR crystal. The apparent enrichment of HPMC at the ATR crystal interface cannot be explained purely by changes in surface activity. Firstly there is a length scale mismatch between the effective sampling depth of the ATR experiment and interfacial molecular adsorption phenomena. Secondly, experiments in similar systems (Reidl et al. [37]) have shown that there is an apparent increase in surface tension at the gelation point, rather than the decrease which might be expected from increased surface activity. This is consistent with our experience of phase separation at the gel point being associated with increased viscoelastic properties, with the resulting tackiness compromising the utility of classic surface tension measurements.

The data shown in Fig. 4 indicate that the intensity of the infrared bands of water are significantly reduced as a function

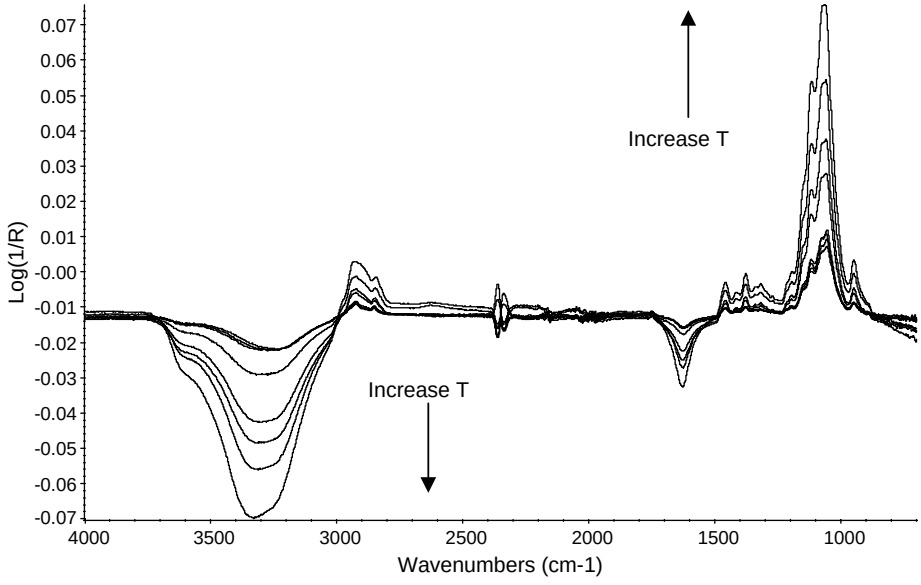

Fig. 4. Changes in band the intensities of the ATR-FTIR spectra of a 2% E4M solution as a function of T.

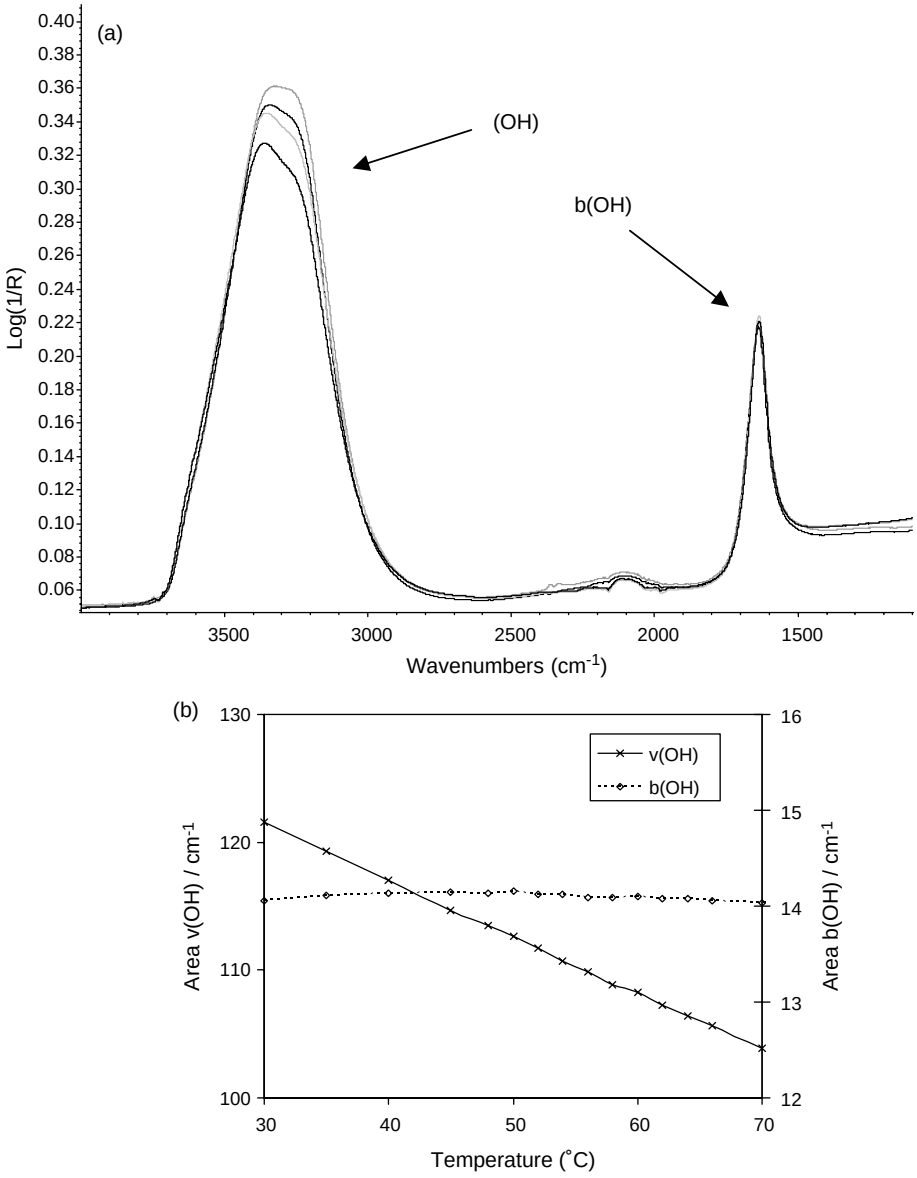

Fig. 5. (a) FTIR-ATR spectra of pure water at 30, 40, 50 and 60 °C and (b) plot of integrated intensity of ν(OH) and b(OH) bands of pure water in (a).

of T. The ν(OH) band of water is highly sensitive to temperature, with changes in shape and intensity observed at different temperatures, but in liquid water, the bending mode has been shown to be insensitive to such changes [36]. Experimentally this is trivial to show. Fig. 5(a) shows the changes in the FTIR-ATR spectrum of pure water at 30, 40, 50 and 60 °C (in the same cell, under the same conditions as the E4M solutions were studied). Integration of the peak areas of the stretching ($\sim$3400 cm^{-1}) and bending modes ($\sim$1630 cm^{-1}) of pure water as a function of temperature are shown in Fig. 5(b) and emphasises the fact that the intensity (and peak position) of the OH stretching mode is highly sensitive to changes in temperature, whilst the intensity of the OH bending mode is essentially independent of temperature. Therefore, we can conclude that a reduction in the intensity of the b(OH) in Fig. 4 must be related to the reduction in the concentration of water at the evanescent field and is therefore evidence of syneresis.

Additional information regarding the interactions between the polymer chains and water within the gel network can also be elucidated from the ATR-FTIR spectra. For example, there are significant changes in the shape of the ν(OH) band during gelation. This data was collected by ratioing the sample single beam against the single beam of pure water at the same temperature to remove the contribution of the bulk water. In principle, changes in band shape associated with temperature should also be removed and differences in the ν(OH) band shape can be related to modifications of the water hydrogen bond network in the gel. From the shape of the ν(OH) band (negative band around 3400 cm^{-1} shown in Fig. 4) it is clear that the water in the gel is somewhat differently organised compared with the water in the solution. This can be investigated in more detail by modelling the changes in the

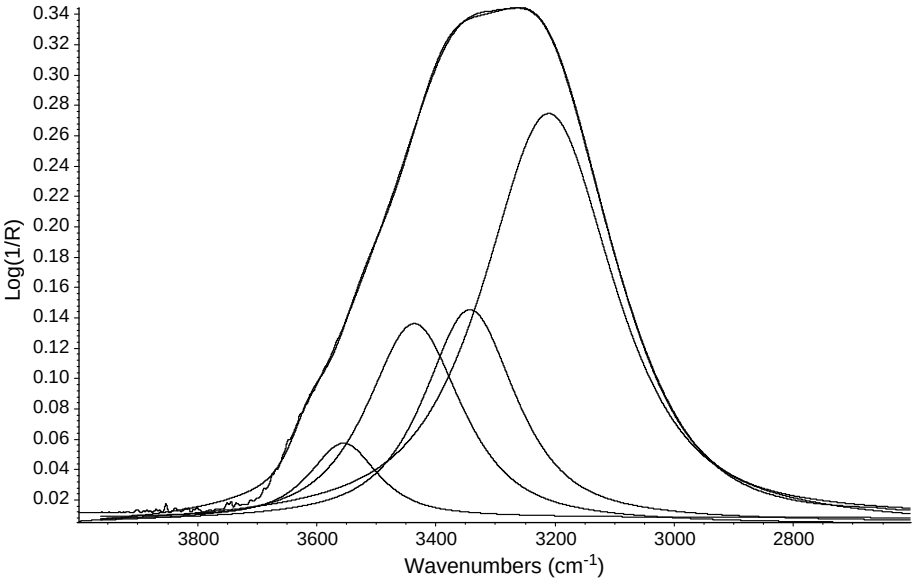

Fig. 6. The ν(OH) of pure water at 40 °C fitted to four mixed Gaussian (20%)/Lorentzian (80%) peaks.

ν(OH) band. It is worth highlighting the nature of the OH stretch to help justify this comment. In Fig. 4, as previously stated, each spectrum shown is the result of the log, of the result of ratioing the single beam of the polymer solution against the single beam of pure water at the same temperature. In this case any band that is negative in the spectrum is therefore of lower concentration in the polymer solution/gel than the pure water reference. We have previously shown, for similar systems, that there is insufficient change in the refractive index of the polymer solution/gel as a function of temperature to impact on the effective path length (i.e. dp, see Eq. (1)) during the heating experiment [36]. As the polymer solution is 2% HPMC by weight at the start of the experiment, it is of no surprise that the bands associated with water are negative; by definition there is 2% less water in the evanescent field in the polymer solution than pure water. But clearly as the temperature is raised additional changes to both the intensity (the result of syneresis) and band shape (the result of reorganisation of the water in the gel) were observed. As changes in water hydrogen bonding strength have been widely studied [20–25] we can readily interpret these changes.

Fig. 6 shows the result of fitting the ν(OH) band of pure water at 30 °C to four peaks with centres around 3610, 3520, 3390 and 3215 cm^{-1}, described previously by Sammon et al. [38] as weakly-, moderately weakly-, moderately strongly- and strongly-hydrogen bonded water, in agreement with the chemometric studies of Libnau et al. [23,24]. Changing the hydrogen bonding structure of the water will modify the ratio of these different components, resulting in a different band shape. Conversely, simply reducing the concentration of water will merely reduce the intensity of the bands by a proportion related to that concentration. Simulations of the resultant ν(OH) gel band shape were made in the following way; changes in the relative intensities of the four component bands of pure water were made to create a synthetic water spectrum. The inverse log of the synthetic water spectrum was ratioed against the inverse log of the real water spectrum. The plot of the log of this 'ratio' versus wavenumber will be referred to in the rest of this text as a 'model ν(OH) gel band'. Fig. 7 shows the comparison of two model ν(OH) gel bands, with the real ν(OH) gel band. There is of course a component associated with the ν(CH) HPMC bands around 2900 cm^{-1} in the real gel spectrum (b) but that has not been considered to impact on the shape of the ν(OH) gel band. The plot labelled (a) shows a simple 80% reduction in all of the four component peaks. Clearly this lacks the detailed 'structure' that is observed in the gel peak (labelled (b)). Plot (c) shows the result of modifying the intensity of the four peaks by 50, 80, 75 and 68%, respectively. This results in a similar band profile and indicates that there is a greater reduction in the intensity of the weakly hydrogen bonded component, which initially seems counter intuitive. One might easily anticipate an increase in the number of weakly hydrogen bonded species in the gel compared with pure water at the same temperature. The obvious inference from this finding is that the water expelled from within the polymer chains is that not hydrogen bonded to the polymer, which is as one may expect. The other observed band intensity changes indicate that relatively the intensities of the bands show the following trend; moderately weak > moderately strong > strong hydrogen bonding. This supports the idea that water within the gel is less strongly hydrogen bonded than pure water, and, given the amphiphilic nature of the polymer this is not unexpected (Fig. 7).

The integrated area of the ν(CO) band as a function of temperature is shown in Fig. 8. There is a clear and distinct increase in intensity as a function of T that begins at 56 °C, the same temperature as a thermal event observed in the DSC measurements and the point at which tan δ is equal to unity in the oscillatory rheometry measurements. Therefore we must conclude that these changes are related to the formation of a gel. In agreement with both the rheology and DSC measurements the cooling curve indicates evidence of

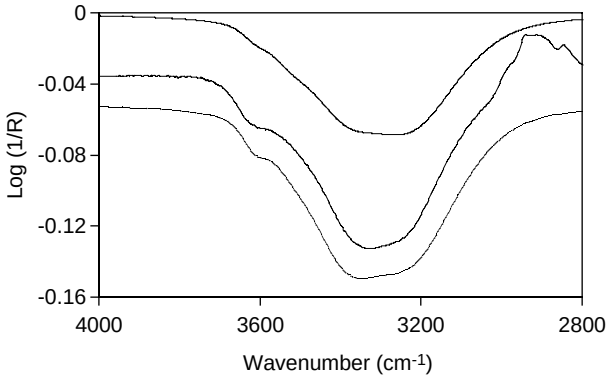

Fig. 7. Comparison of real and modelled data for the ν(OH) region of an HPMC gel rationed against pure water at the same temperature: (a) all peaks 80% of the original intensity, (b) real data and (c) model data with peaks 50, 80, 73 and 68% of their original intensity. Data are off-set for clarity.

hysteresis, further supporting the assertion that the source of the intensity changes is related to the gelation process.

In an attempt to quantify the changes in concentration of water within the gel layer a partial least squares method was applied. Samples of 2, 5, 10, 20 and 30% (w/w) of E4M solution were prepared using the methods outlined by Banks [36]. Spectra from these samples were then recorded in triplicate, with two spectra of each sample concentration being used to generate the calibration plot (10 in total) and the other spectrum at that concentration being used to validate the model (5 in total). To generate the PLS model the region of the FTIR spectrum between 1800 and 700 cm^{-1} was used to avoid errors associated with changing intensities in the ν(OH) band that we have shown relate to the temperature at which the data were collected. Two principal components were found to be sufficient to describe the variation in the data set and the plot of the actual versus calculated concentrations for both E4M HPMC and water are shown in Fig. 9. Fig. 9 shows that the model describes the concentration of the two components rather well with an R^2 value better than 0.99 for both cases.

This model was then used to generate actual concentration plots for water in the evanescent field for 2 and 5% HPMC solutions as a function of temperature (Fig. 10). For the 2% solution, this is based on the same 'heating' data previously shown in Fig. 8. It is interesting to note that for the solutions with initial HPMC concentrations of 2 and 5% of HPMC, the apparent water concentration at the gel/ATR crystal interface at 75 °C is quite similar ~80%, which indicates a significant degree of syneresis and lends credence to the supposition that the increase in the intensity of the polymer bands in the ATR-FTIR data as a function of time are due to an enrichment of HPMC at the ATR crystal interface. Perhaps rather puzzlingly the concentration profile shown in Fig. 10 is not quite an inversion of the shape of the peak area profile shown in Fig. 8. This is almost certainly due to the different methods by which the data were obtained. The peak area profile used the

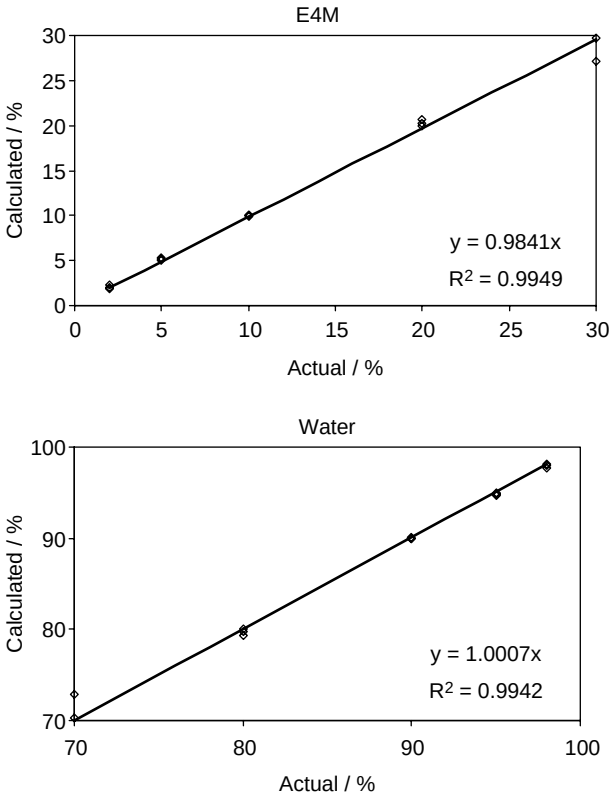

Fig. 9. Actual versus calculated plots showing the fit of the PLS model.

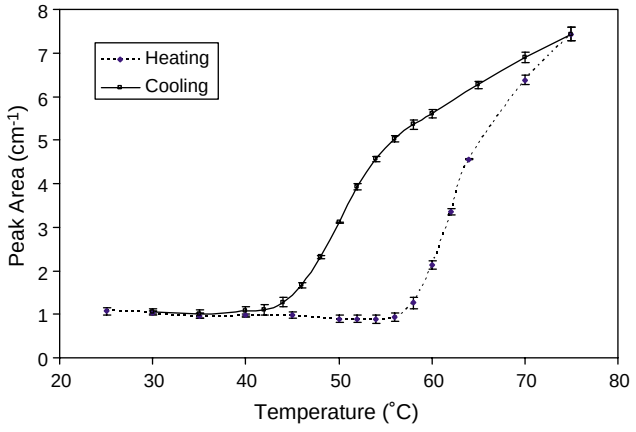

Fig. 8. Integrated area of the ν(CO) band of a 2% E4M solution as a function of T.

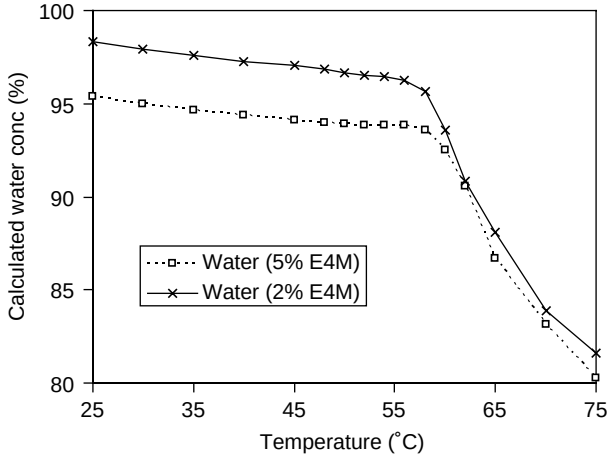

Fig. 10. Calculated water concentration in gel as a function of temperature.

integrated area between two fixed points, using those points as a baseline and only takes into account the ν(CO) band. Whereas the PLS method takes into account a larger region of the spectrum, that pertains to many different vibrations and includes bands associated with water. One other factor that should be taken into account is that the band shape of the ν(CO) band changes during the gelation process and this may have an effect on the calculated concentration profile. These changes in band shape are the subject on an ongoing investigation and we will report our findings in due course.

4. Conclusions

It has been shown that ATR-FTIR can be applied successfully to monitor thermal gelation processes in HPMC solutions. The onset of thermal gelation is marked by an increase in the intensity of the ν(CO) band at $\sim 1050\ \mathrm{cm}^{-1}$ in the spectrum of the solution. These intensity increases are accompanied by decreases in the intensity of bands associated with water and this we have interpreted as evidence of syneresis. A partial least squares model has been used to quantify the decrease in concentration of water within the gel and some of the limitations of this data have been discussed. The gel point temperature obtained from the ATR-FTIR data was in good agreement with that obtained using two separate methods; differential scanning calorimetry and oscillatory rheometry. The changes in the band shape of the ν(OH) band during gelation indicate a preferred removal of weakly hydrogen bonded water species from between the polymer layers during gelation. The relative ease with which additional information regarding interactions, such as hydrogen bonding, can be elucidated from the spectroscopic data make it a powerful technique for such studies in the future.

References

[1] Sanz T, Salvador A, Fiszman SM. Food Hydrocolloids 2004;18(2): 227–31.
[2] Wang W, Liu YZ, Gu YG. Colloid Polym Sci 2003;281(11):1046–54.
[3] Madhan B, Muralidharan C, Jayakumar R. Biomaterials 2002;23(14): 2841–7.
[4] Rajabi-Siahboomi AR, Bowtell RW, Mansfield P, Henderson A, Davies MC, Melia CD. J Controlled Release 1994;31(2):121–8.
[5] Hirrien M, Chevillard C, Desbrieres J, Axelos MA, Rinaud M. Polymer 1998;39(25):6251–9.
[6] Sekiguchi Y, Sawatari C, Kondo T. Carbohydr Polym 2003;53(2): 145–53.
[7] Kondo T. J Polym Sci Polym Phys 1997;35(4):717–23.
[8] Kondo T, Sawatari C. Polymer 1994;35(20):4423–8.
[9] Kita R, Kaku T, Ohashi H, Kurosu T, Iida M, Yagihara S, et al. Physica A 2003;319:56–64.
[10] Thuresson K, Lindman B. Colloids Surf A 1999;159(1):219–26.
[11] Ostrovskii D, Kjoniksen AL, Nystrom B, Torell LM. Macromolecules 1999;32(5):1534–40.
[12] Lindell K, Cabane B. Langmuir 1998;14(22):6361–70.
[13] Wang G, Lindell K, Olofsson G. Macromolecules 1997;30(1):105–12.
[14] Carlsson A, Karlstrom G, Lindman B. Colloids Surf 1990;47:147–65.
[15] Ford JL. Int J Pharm 1999;179(2):209–28.
[16] Ibbett RN, Philp K, Price DM. Polymer 1992;33(19):4087–94.
[17] Klug ED. J Polym Sci 1971;36:491–508.
[18] Haque A, Morris ER. Carbohydr Polym 1993;22(3):161–73.
[19] Haque A, Richardson RK, Morris ER, Gidley M, Caswell D. Carbohydr Polym 1993;22(3):175–86.
[20] Max JJ, Chapados C. Appl Spectrosc 1999;53(12):1601–9.
[21] Max JJ, de Blois S, Veilleux A, Chapados C. Can J Chem 2001;79:13–21.
[22] Bertie JE, Lan Z. Appl Spectrosc 1995;49(6):840–51.
[23] Libnau FO, Kvalheim OM, Christy A, Toft J. Vib Spectrosc 1994;7(3): 243–54.
[24] Libnau FO, Chrsty AA, Kvalheim OM. Appl Spectrosc 1995;49(10): 1431–7.
[25] Hare DE, Sorensen CM. J Chem Phys 1992;96:13–22.
[26] Harrick NJ. In: Harrick NJ, editor. Internal reflection spectroscopy. New York: Harrick Scientific Corporation; 1987.
[27] Malik S, Nandi AK. J Phys Chem B 2004;108(2):597–604.
[28] Su YL, Liu HZ, Guo C, Wang J. Mol Simulat 2003;29(12):803–8.
[29] Goeden-Wood NL, Keasling JD, Muller SJ. Macromolecules 2003;36(8): 2932–8.
[30] Gosal WS, Clark AH, Pudney PDA, Ross-Murphy SB. Langmuir 2002; 18(19):7174–81.
[31] Iizuka K. T Aishima. J Food Sci 1999;64(4):653–8.
[32] Wilson RH, Kalichevsky MT, Ring SG, Belton PS. Carbohydr Res 1987; 166(1):162–5.
[33] Bulkin BJ, Kwak Y, Dea ICM. Carbohydr Res 1987;160:95–112.
[34] Liu Q, Charlet G, Yelle S, Arul J. Food Res Int 2002;35:397–407.
[35] Ostrovskii D, Kjoniksen A-L, Nystrom B, Torell LM. Macromolecules 1999;32:1534–40.
[36] Banks SR, Sammon C, Melia CD, Timmins P. Appl Spectrosc 2005; 59(4):452–9.
[37] Reidl Z, Szklenárik GY, Zelkó R, Marton S, Rácz I. Drug Dev Ind Pharm 2000;26(12):1321–3.
[38] Sammon C, Yarwood J, Mura C, Everall N, Swart R, Hodge D. J Phys Chem 1998;102:3402–11.